Electrolytic Formation of Carbon-Sheathed Mixed Sn−Pb Nanowires

W. K. Hsu,[†] S. Trasobares,[†] H. Terrones,[‡] M. Terrones,[†] N. Grobert,[†] Y. Q. Zhu,[†] W. Z. Li,[†] R. Escudero,[§] J. P. Hare,[†] H. W. Kroto,[†] and D. R. M. Walton*,[†]

School of Chemistry, Physics and Envirnomental Science, University of Sussex, Brighton BN1 9QJ, U.K., Instituto de Fisica, UNAM, Apartado Postal 20-364, D.F.01000, Mexico, and Instituto de Investigaciones en Materiales, UNAM, Apartado Postal 70-360, D.F.01000, Mexico

Received December 14, 1998. Revised Manuscript Received April 12, 1999

Carbon-encapsulated Sn−Pb nanowires are generated by electrolysis of graphite in molten LiCl containing these metals. SA-EDX analyses indicate a distinctive profile for the metal cores in which Sn predominates at one end and Pb at the other of the individual nanowires; X-ray diffraction measurements reveal that separate crystals of each metal can be distinguished, thus zone refining has occurred. The cores exhibit dynamic behavior under electron irradiation. A growth mechanism is proposed for the nanowires.

Introduction

Low-dimensional (i.e., 1D or 2D) metal-like conductors exhibit electron transport properties which differ from those observed in the bulk phase. For example, the ballistic behavior, which occurs when the dimensions of the conductor are comparable with that of the mean free path of an electron, results in stepwise conductance at low temperature.[1,2] As a consequence of experiments carried out on pure carbon nanotubes, well-defined quantum wire behavior has been identified at 5 mK for single-walled carbon nanotubes (SWNTs),[3] and regular conductance jumps ($2e^2/h$) recorded at room temperature for multiwalled carbon nanotubes (MWNTs).[4] The fabrication of such conducting structures, e.g., quantum dots,[5] GaAs−AlGaAs heterojunctions for a 2-D electron gas,[6] and the formation of restricted conduction by STM tips in contact with a metallic substrate,[7] has proved to be a fascinating topic for over a decade.

Recently, metallic nanowires, coated with carbon or other materials (e.g., BN and SiO_2) have been produced by vapor−solid reactions and by laser ablation techniques.[8−11] In previous reports, we described the production of metal nanowires by the electrolysis of graphite in the presence of a molten salt (LiCl) and doped with various trace metals (e.g., Bi, Pb, and Sn).[12,13] The formation mechanism may involve electrodeposition of

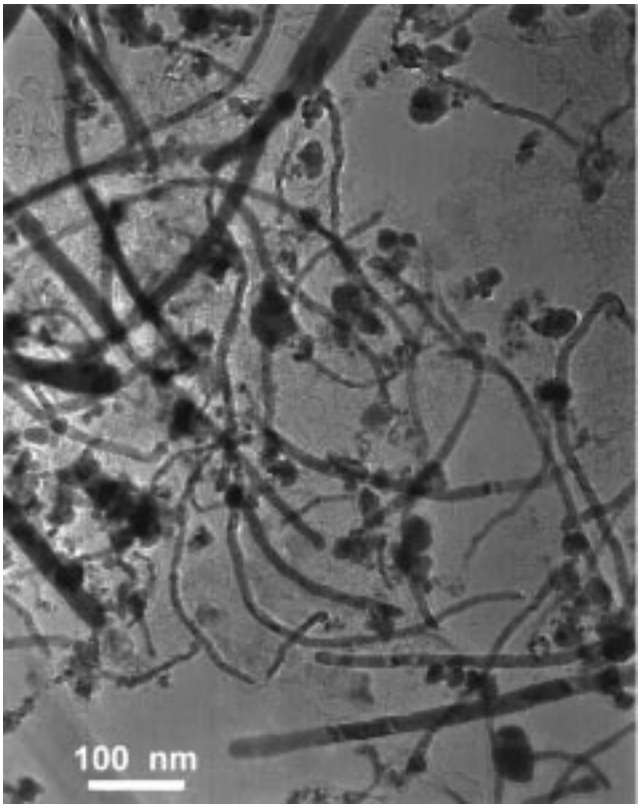

Figure 1. TEM image of electrolytically generated Sn−Pb nanowires.

[†] University of Sussex.
[‡] Instituto de Fisica, UNAM.
[§] Instituto de Investigaciones en Materiales, UNAM.

(1) Sharvin, Yu. V. *J. Exptl. Theor. Phys. (U.S.S.R.)* **1965**, *48*, 984−985.
(2) van Wees, B. J.; Van Houten, H.; Beenakker, C. W. J.; Williamson, J. G.; Foxon, C. T. *Phys. Rev. Lett.* **1988**, *60*, 848−850.
(3) Tans, S. J.; Devoret, M. H.; Dai, H. J.; Thess, A.; Smalley, R. E.; Geerligs, L. J.; Dekker, C. *Nature* **1997**, *386*, 474−476.
(4) Frank, S.; Poncharal, P.; Wang, Z. L.; De Heer, W. A. *Science* **1998**, *280*, 1744−1746.
(5) Dingle, R.; Wiegmann, W.; Henry, C. H. *Phys. Rev. Lett.* **1974**, *33*, 827−830.
(6) Thornton, T. J.; Pepper, M.; Ahmed, H.; Andrews, D.; Davies, G. J. *Phys. Rev. Lett.* **1986**, *56*, 1198−1201.
(7) Gimzewski, J. K.; Möller, R. *Phys. Res.* **1987**, *B36*, 1284−1286.
(8) Dai, H. J.; Wong, E. W.; Lu, Y. Z.; Fan, S. S.; Lieber, C. M. *Nature* **1995**, *375*, 769−771.
(9) Han, W.; Fan, H.; Li, Q.; Hu, Y. D. *Science* **1997**, *277*, 1287−1290.
(10) Morales, A. M.; Lieber, C. M. *Science* **1998**, *279*, 208−210.
(11) Zhang, Y.; Suenaga, K.; Colliex, C.; Iijima, S. *Science* **1998**, *281*, 973−975.
(12) Hsu, W. K.; Terrones, M.; Terrones, H.; Grobert, N.; Kirkland, A. I.; Hare, J. P.; Prassides, K.; Townsend, P. D.; Kroto, H. W.; Walton, D. R. M. *Chem. Phys. Lett.* **1998**, *284*, 177−180.

10.1021/cm981127e CCC: $18.00
Published on Web 06/04/1999

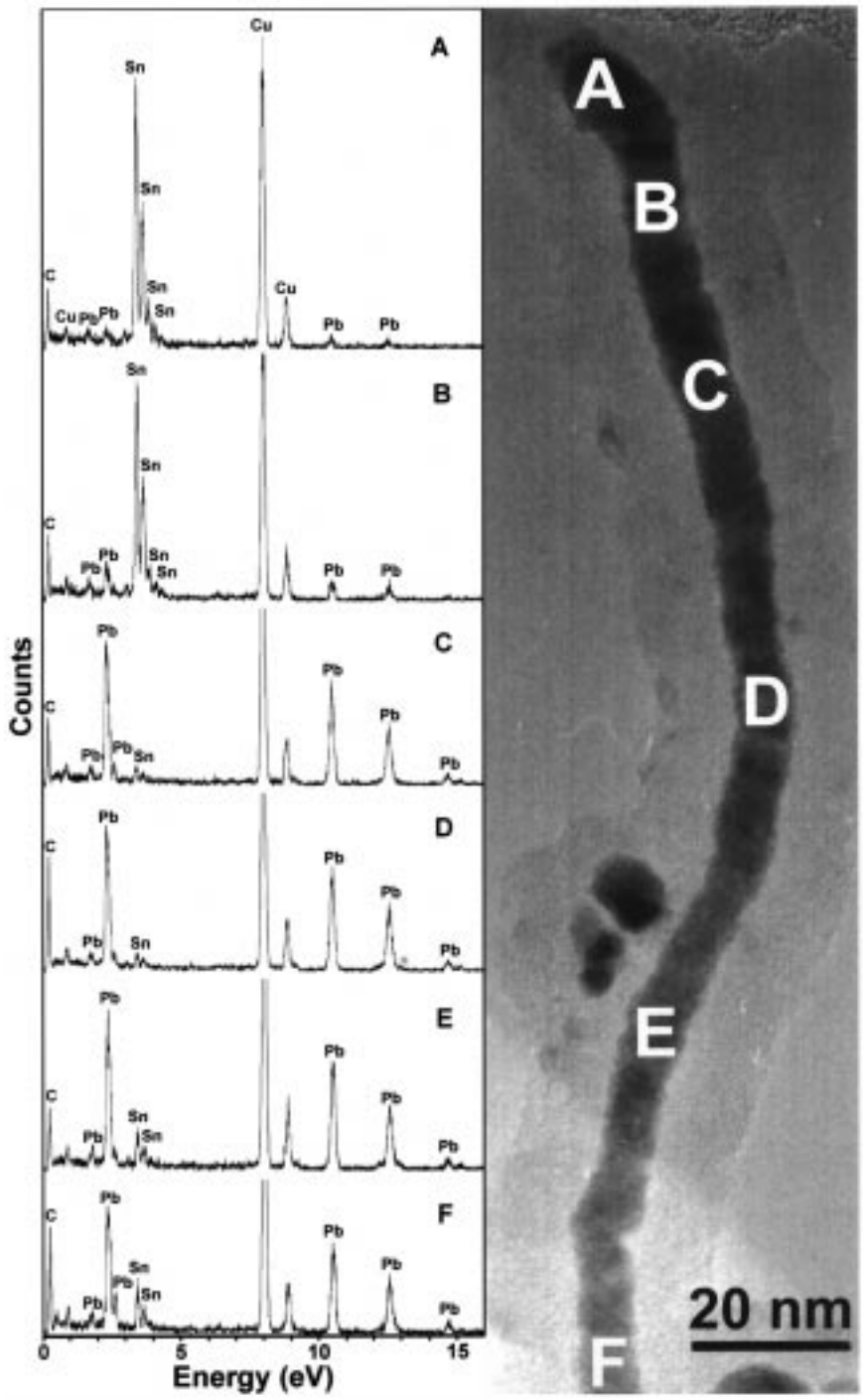

Figure 2. EDX analyses of a Sn−Pb nanowire. The letters A, B, C, D, E, and F along the wire axis represent positions at which the EDX spectrum was recorded. C signal arises from the carbon walls of Pb−Sn nanowires and Cu signals originated from the TEM Cu grid. The area F is located ~2 nm from the end of the nanowire.

metal at the cathode, providing a site for nanowire formation. In this paper, we describe a related series of experiments using a mixed LiCl/Sn/Pb electrolyte in which mixed Pb−Sn nanowires are generated in high yield.

Experimental Section

The electrolytic cell and operating conditions have been described.[14,15] The electrolyte (~50 g) was prepared by mixing LiCl with small amount of Sn and Pb (99% + 0.5% +0.5 wt %, respectively) and the graphite cathode (3-mm diameter) immersion depth in the electrolyte was set at 2 cm. The current was varied by carefully by adjusting the voltage (0−20 V at 3−7 A) and, for the sake of uniformity, was maintained for 2 min in each experiment (the melt was maintained at 600 °C). After electrolysis, the nanowire samples were extracted as described previously[14,15] and examined using high-resolution transmission electron microscopes [HRTEM, JEOL-4000FX (400keV) and JEOL-2010 200keV)] equipped with X-ray detec-

(13) Hsu, W. K.; Li, J.; Terrones, M.; Terrones, H.; Grobert, N.; Hare, J. P.; Kroto, H. W.; Walton, D. R. M. *Chem. Phys. Lett.* **1999**, *301*, 159.

(14) Hsu, W. K.; Hare, J. P.; Terrones, M.; Kroto, H. W.; Walton, D. R. M.; Harris, P. J. F. *Nature* **1995**, *377*, 687.

(15) Hsu, W. K.; Terrones, M.; Hare, J. P.; Terrones, H.; Kroto, H. W.; Walton, D. R. M. *Chem. Phys. Lett.* **1996**, *262*, 161−164.

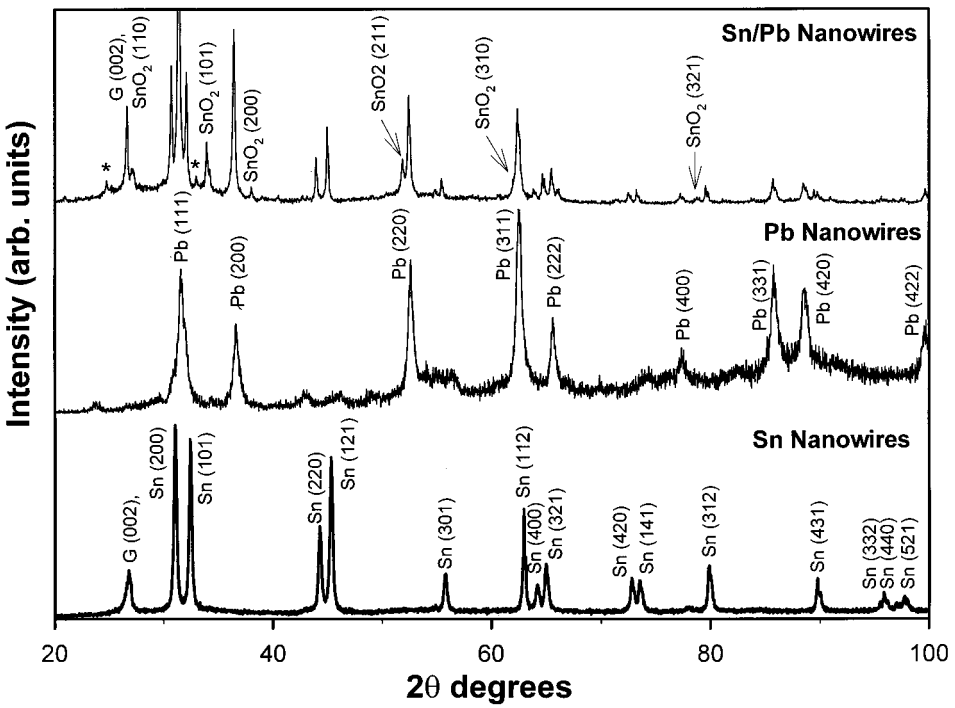

Figure 3. X-ray diffraction of Sn−Pb nanowires (top) compared with Pb nanowires (middle) and Sn nanowires (bottom). The SnO_2 reflections (denoted by arrows) arise from residual unreacted Sn, and the minor star peaks cannot be identified. (EDX analyses showed that oxygen is absent from the nanowires). Compared with a single metal (Pb or Sn), the lattice parameter for Pb−Sn nanowires remained unchanged.

Table 1. Sn:Pb Ratios Calculated from Figure 2[a]

	spectra recorded positions from Figure 2					
	A	B	C	D	E	F
Sn:Pb ratios	91.8:8.2	81.4:18.6	6.63:93.4	4.9:95.1	10.8:89.2	15.8:84.2

[a] The Sn:Pb ratios were calculated from the intensities of L and M shell (counts) and the error ($1 - \sigma$) is ±200.

tors (Si/Li type). The duration of the EDX scans on individual wires was 20−40 s.

Results

Figure 1 shows a TEM image of nanowires generated by electrolysis, ranging from 4 to 7 μm in length and 40−90 nm in diameter. The yield is roughly estimated to be approximately 40−60%, on the basis of TEM observations. To evaluate the composition, selective-area energy-dispersive X-ray analyses (SA-EDX) were carried out on 10 selected individual nanowires, which were scanned along their length, and spectra were recorded section by section. The presence of a binary phase (Sn−Pb) was confirmed for nine nanowires; the 10th nanowire contained only Pb. Unexpectedly, the Sn:Pb ratio was found to vary considerably from one end of each nanowire to the other, with slight variations from one wire to another. A representative nanowire is shown in Figure 2 (see also Table 1). The intensity of the Pb spectrum increases from the top (∼84%) to bottom (∼8%) as the percentage of Sn decreases in relative proportion. To demonstrate that the Sn−Pb nanowires constitutes a major proportion of the material, EDX analyses were carried out on six additional nanowires, and their spectra were also recorded selectively (Table 2). Our study shows that approximately 70−80% Sn and 80−90% Pb are located at either end of the nanowire,

Table 2. Sn:Pb Ratios for Six Additional Nanowires

	selective area			
	one end	$^1/_3$	$^2/_3$	other end
nanowire 1	92.8:7.2	96.9:3.1	93.4:6.6	6.2:93.8
nanowire 2	22.46:77.54	*a*	4.9:95.1	8.2:91.8
nanowire 3	66.4:33.6	6.7:93.3	7.9:92.1	3.9:96.1
nanowire 4	90:10	7.9:92.1	*a*	7.7:92.3
nanowire 5	*a*	*a*	12.5:87.5	*a*
nanowire 6	*a*	*a*	*a*	2.1:97.9

[a] Unrecorded.

but that the relative metal content fluctuates considerably in the central nanowire sections. During electrolysis, we applied a 6−7 A current to the system which resulted in preferential generation of such Sn−Pb nanowires. The Sn or Pb metal enrichment at the end of the nanowire becomes indistinguishable when electrolysis was undertaken at 3−4 A. It is also noteworthy that when a nanowire possesses an uneven cross-section, the Pb level is always greater in the thicker section. This phenomenon is shown in Table 2 (nanowire 6), in which the nanowire has an uneven cross-section containing Pb (98%) at the thicker end.

Sn−Pb alloy is a well-known solid solution system (containing 63% Sn by weight)[16] with an eutectic temperature of 183 °C. X-ray diffraction measurements in our experiments however show well-separated Sn (tetragonal) and Pb (fcc) crystal structures (Figure 3). Note that X-ray diffraction measurements cannot accurately determine the existence of a varied crystal structure caused by the presence of a few impurity atoms (intermetallic domains).[19] For example, Pb can maintain a

(16) Hedges, E. S., Ed. *Tin and Its Alloys*; Edward Arnold. Ltd.: London, 1960; pp 334−337.
(17) Smith, D. J.; Petford-Long, A. K.; Wallenberg, L. R.; Bovin, J. O. *Science* **1986**, *233*, 872−875.

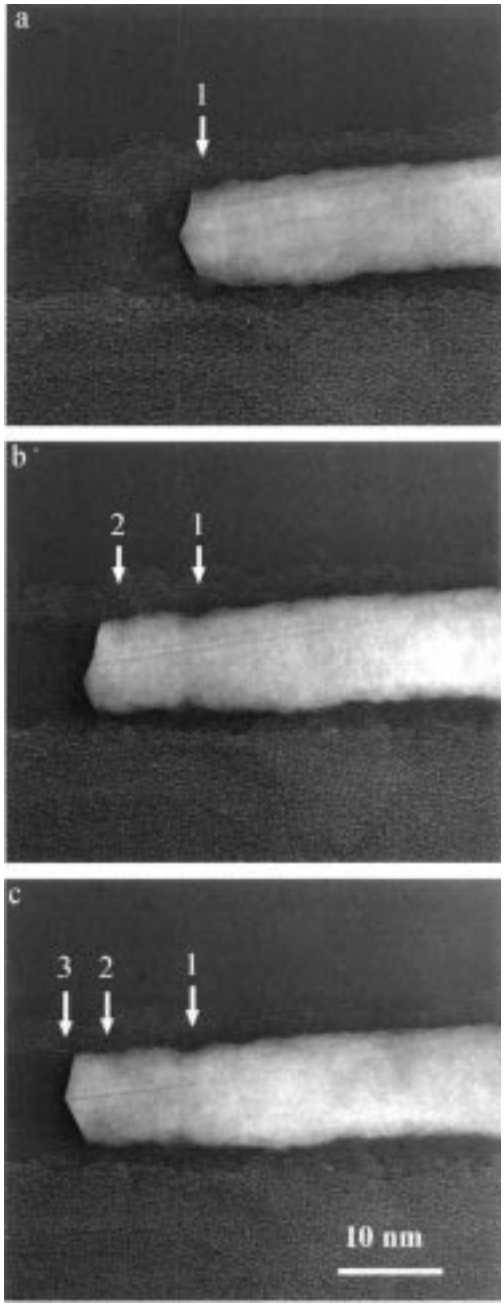

Figure 4. HRTEM images (dark field) of the transformation sequence for endohedral Sn−Pb caused by electron irradiation: (a) cone-like structure changed into asysmmetrical cap; (b) after 50-s irradiation, the endohedral alloy has moved (∼10 nm) along the wire axis (marked by arrow 1-2); after a further 60 s, a larger cone-shaped modification has emerged (c), and the Sn−Pb wire has moved another ∼5 nm (marked by arrow 2-3).

fcc phase in the presence of a few Sn atoms,[19] and variable crystal structures may exist at the Sn−Pb grain boundaries.

In a previous study, dynamic behavior of metals (Sn or Pb) encapsulated in carbon under electron beam irradiation (400 keV) was observed.[12] Similar behavior also occurs in Sn−Pb nanowires (Figure 4a−c). Here, the original cone structure (Figure 4a) transforms into

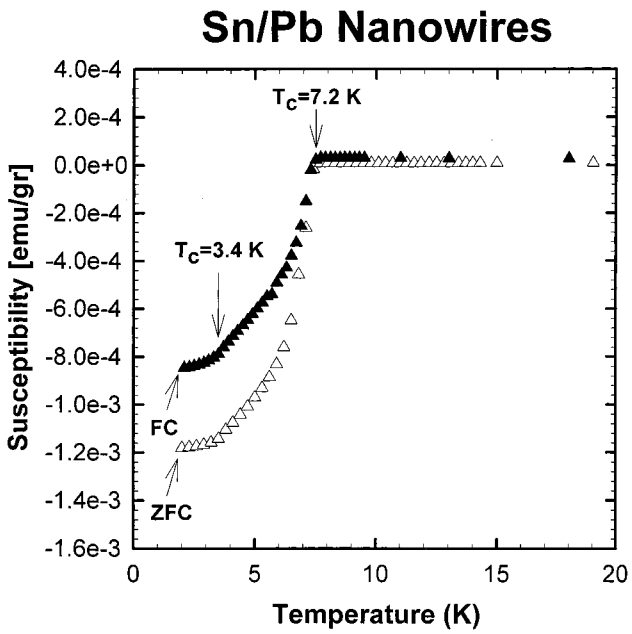

Figure 5. SQUID data for the Sn−Pb nanowires, $T_c = 7.2$ K for Pb and $T_c = 3.4$ K for Sn. The results are similar to that of the bulk phase.

an asymmetric cap (Figure 4b) after ∼50 s of irradiation. Meanwhile, the encapsulated material moves ∼10 nm along the wire axis (denoted by arrows). The nanowire then becomes cone-like again (Figure 4c) and the Sn−Pb slugs move ∼5 nm after another 60 s of irradiation. The crystal plane lattices are changing during the course of this transformation (Figure 4, parts a and c). Atomic rearrangements caused by heating (inelastic scattering) and the knock-on effect of atomic displacements (momentum transfer) have been demonstrated for small metal clusters (∼10−30 Å).[17,18] This suggests that the shapes of metal particles associated with the supporting substrate (silica or carbon) may play a role in determining dynamic behavior, e.g., the contact angle and the path for heat dissipation. In this study, the encapsulated metals are encased in carbon tubes and are therefore isolated from the holey carbon support film. The contact angle between metals and carbon is more or less uniform. Thus, the metals provide an efficient route for heat dissipation, suggesting that the thermal effect should be less important. The dynamic behavior observed here could thus be caused by the knock-on effect.

The origin of the change in physical properties (e.g., superconductivity) due to the size effect and/or variation in chemical composition of the materials is a well-known issue. Figure 5 shows the result of SQUID measurements for the Sn−Pb nanowires, in which $T_c = 7.2$ K for Pb and $T_c = 3.4$ K for Sn. In this study, Sn−Pb nanowires exhibit superconducting behavior similar to that of the bulk material (i.e., size and chemical effects are absent in our samples); however, the susceptibility decreases slowly for reasons which are not clear.

In addition to the Sn−Pb nanowires, ∼20−30% of the produced material consists of roughly spherical carbon-coated metallic particles (5−30 nm in diameter). EDX analyses revealed the presence of one or other metal (Sn or Pb) in these particles; only rarely was a binary phase detected and then only in the larger (∼25−30 nm) particles.

(18) Iijima, S.; Ichihashi, T. *Phys. Rev. Lett.* **1986**, *56*, 616−620.
(19) Parr, N. L. *Zone Refining and Allied Techniques*; George Newnes Ltd.: London, 1960; pp 1−6.

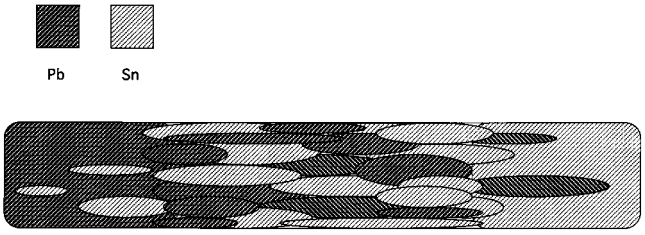

Figure 6. Structure of the observed Sn−Pb nanowire.

In similar experiments using LiCl/Bi/Pb and LiCl/Sn/Bi mixtures as electrolytes, the preferential formation of roughly spheroidal carbon-coated metallic particles (approximately >70%) and amorphous carbon material (∼20−25%) were observed, and the nanowire yield was low (approximately <5%). EDX analyses indicated the presence of a single metal (Pb, Sn, or Bi) in the nanowires and particles; a trace of binary phase (Bi−Pb or Sn−Bi) was occasionally detected in the thicker nanowires or larger particles. Selective metal enrichment at the ends of the nanowires was not observed.

Discussion

Figure 6, based on EDX analyses, illustrates the observed Sn−Pb nanowires, and a mechanism proposed in our earlier paper, to account for nanotube and metal nanowire formation, remains valid. (That is, the adsorption of Li_2C_2 on the liberated Sn and Pb metal globules which may catalyze the self-assembly of carbon-sheathed nanowires. The Sn−Pb mixture is deposited at the tip of a growing dendrimer by electrons furnished by adsorption and oxidation of Li_2C_2 along with the growing conducting carbon sheath.[13]) The question remains as to why Sn enrichment occurs at the ends of the wires, since Sn and Pb were initially added in equal amounts, by weight, to the electrolyte (LiCl). Here we propose a mechanism which combines the metal encapsulation (proposed previously[13]) with a "zone refining" type process.[19] On the basis of our previous study, the yields of Sn and Pb nanowires created by electrolysis are comparable (∼40−50%), therefore one would expect both metals to be encapsulated during the process with roughly equal probability. This implies that "zone refining" plays a crucial role in the generation of a nonequilibrium metal phase. When metals solidify, crystal development is controlled by adjacent growing crystals or expitaxial constraints. The dispersed insoluble impurities in the molten metal will be forced along the growing crystals. Such a process is used to purify materials. As the temperature decreases, the first metal to precipitate from a eutectic alloy (e.g. Sn−Pb) is the metal with the higher melting point (mp). According to time versus temperature solidification studies, zone refining can occur if the temperature is set above the eutectic temperature, and pure metal so produced.[19] [The zone refining process is carried out industrially using a narrow heating zone (temperature set above the eutectic) which allows passage of the molten alloy in one direction.] In this case, when Sn−Pb droplets are trapped inside the carbon tubes and the metal−metal ratio may be maintained at a level more or less the same as in the electrolyte. Larger currents (6−7 A) would generate significant localized temperature gradients near the cathode in the domains where zone refining occurs. The observations suggest that Pb (mp 320 °C) precipitates first as the wire grows and Sn (mp 232 °C) precipitates subsequently, initially together with Pb, in the central section of the tubule (Figure 6). Sn continues to precipitate as Pb is "zone refined". Segregation processes do not appear to occur to any significant extent during the formation of small particles containing encapsulated metals.

The preferential formation of metal-encapsulated particles rather than nanowires, when the electrolyte consisted of LiCl/Bi/Sn or LiCl/Pb/Bi, may simply reflect the characteristics of the nonsolid/solution system.

Acknowledgment. We thank the EPSRC (J.P.H.), the Royal Society (W.K.H., Y.Q.Z., and M.T.), DERA Malvern and the JFCC (N.G.), Conacyt-Mexico, DGAPA-UNAM IN-107-296 (H.T.), and DGA CAI-CONSI + D (S.T.) for finacial support.

CM981127E